Applications of Mathematics

Lu Zou; Yuan Lei

The descent algorithms for solving symmetric Pareto eigenvalue complementarity problem

Applications of Mathematics, Vol. 68 (2023), No. 4, 441–465

Persistent URL: http://dml.cz/dmlcz/151704

Terms of use:

© Institute of Mathematics AS CR, 2023

Institute of Mathematics of the Czech Academy of Sciences provides access to digitized documents strictly for personal use. Each copy of any part of this document must contain these *Terms of use*.

This document has been digitized, optimized for electronic delivery and stamped with digital signature within the project *DML-CZ: The Czech Digital Mathematics Library* http://dml.cz

THE DESCENT ALGORITHMS FOR SOLVING SYMMETRIC PARETO EIGENVALUE COMPLEMENTARITY PROBLEM

LU ZOU, YUAN LEI, Changsha

Received January 28, 2022. Published online February 3, 2023.

Abstract. For the symmetric Pareto Eigenvalue Complementarity Problem (EiCP), by reformulating it as a constrained optimization problem on a differentiable Rayleigh quotient function, we present a class of descent methods and prove their convergence. The main features include: using nonlinear complementarity functions (NCP functions) and Rayleigh quotient gradient as the descent direction, and determining the step size with exact linear search. In addition, these algorithms are further extended to solve the Generalized Eigenvalue Complementarity Problem (GEiCP) derived from unilateral friction elastic systems. Numerical experiments show the efficiency of the proposed methods compared to the projected steepest descent method with less CPU time.

Keywords: Pareto eigenvalue complementarity problem; generalized eigenvalue complementarity problem; nonlinear complementarity function; descent algorithm

MSC 2020: 65F10, 65F20, 65F22, 65K10

1. INTRODUCTION

The Eigenvalue Complementarity Problem (EiCP) is a special kind of complementary problem, also known as the cone-constrained eigenvalue problem, which consists of finding a scalar $\lambda \in \mathbb{R}$ and a nonzero vector $x \in \mathbb{R}^n$ such that

$$x \in K, \quad Ax - \lambda Bx \in K^+, \quad \langle x, Ax - \lambda Bx \rangle = 0, \tag{1.1}$$

where real matrix $A, B \in \mathbb{R}^{n \times n}$ and $K \subset \mathbb{R}^n$ is a closed convex cone. The notation $K^+ = \{y \in \mathbb{R}^n \mid \langle x, y \rangle \geqslant 0 \text{ for all } x \in K\}$ stands for the dual cone of K, see [3]. The Eigenvalue Complementarity Problem was originally derived from the

This research is partially supported by the National Natural Science Foundation of China (No. 11871205).

DOI: 10.21136/AM.2023.0020-22

© Institute of Mathematics, Czech Academy of Sciences 2023.

study of variational inequality operators based on bifurcation theory [10], [20], [7], [11], [21], [9]. The mathematical theory of EiCP together with its numerical method for computing eigenvalues and eigenvectors are extensively employed in the stability analysis of frictional elastic systems and acoustic systems, the dynamic analysis of structural mechanical systems, and fluid dynamics, among other scientific and engineering fields [14], [15], [16], [17], [26]. Generally speaking, the eigenvalues for a given real matrix are inconsistent under the constraints of cones with varied structures, as are their theoretical properties. When $K = \mathbb{R}^n$, its dual cone degenerates to zero, i.e., $K^+ = \{0\}$, and the EiCP is then turned into a classical matrix eigenvalue problem [22]. As a consequence, the EiCP is a generalization of the classical matrix eigenvalue problem. However, many theoretical properties of the classical matrix eigenvalue problem cannot be extended to the EiCP, such as similarity invariance, transpose invariance, and so on. Therefore, due to the wide applicability and complexity of the Eigenvalue Complementarity Problem, it has rapidly become one of the research hotspots in the field of scientific computing in recent years.

This paper focuses on the eigenvalue complementarity problem on a class of self-dual cones (non-negative cone $K = \mathbb{R}^n_+$) [25], namely the Pareto EiCP, which can be described as follows: Given real matrices $A, B \in \mathbb{R}^{n\times n}$, find a scalar $\lambda \in \mathbb{R}$ and a nonzero vector $x \in \mathbb{R}^n$ to satisfy

$$(1.2) \qquad x \geqslant 0, \quad Ax - \lambda Bx \geqslant 0, \quad \langle x, Ax - \lambda Bx\rangle = 0;$$

we use the notation EiCP(A, B) to denote an EiCP with given matrices A and B. For the scalar λ and the nonzero vector x that satisfies system (1.2), we call them Pareto eigenvalue and associated Pareto eigenvector of the given pair (A, B), respectively.

The existence of a solution to the eigenvalue complementarity problem [22] and the number of eigenvalues for the non-negative cone constrained eigenvalue complementarity problem [18] have been theoretically proven. It is noteworthy that the number of Pareto eigenvalues may increase exponentially with the scale of the problem. For example, the number of Pareto eigenvalues for a matrix of order 25 can be as high as 3 million. Moreover, it can be shown that solving all Pareto eigenvalues of large-scale matrices is an NP-hard problem [18], [24], which is a great challenging task in eigenvalue calculation. In terms of numerical solution, the mainstream method currently adopted is to use the nonlinear complementarity function (NCP function) [5], [6] or the projection operator on the cone to equivalently transform the Pareto EiCP into the solution of a nonlinear system of equations $\phi(z) = 0$ consisting of $2n - 1$ equations. If the nonlinear function $\phi(z)$ is semi-smooth at the zeros $\tilde{z}$ and the matrices in the generalized Jacobian $\partial\phi(\tilde{z})$ are nonsingular, the classical semi-smooth Newton method [1], [2] can be utilized. When the generalized Jacobian $\partial\phi(\tilde{z})$ contains a singular matrix, the problem can be transformed into an equivalent unconstrained minimization problem where the objective function is a smooth value function associated with the NCP function [13].

The EiCP of symmetric matrices has a lot of good theoretical properties, such as having a finite number of eigenvalues under the second-order cone constraint [22]. Under simple constraints, the symmetric EiCP can be equivalently transformed into the generalized Rayleigh quotient maximization problem [8], [19], with any stable point of the problem being an eigenvalue of the corresponding complementarity problem, and so can be solved using numerous optimization algorithms [9], [19]. Also for general symmetric matrices, the generalized Rayleigh quotient function is usually nonconvex, but it can be expressed as the difference between two convex functions, so it can also be solved using DC programming methods [12].

Based on the prior literature and our discussions, we mainly focus our efforts on investigating the theory of symmetric Pareto EiCP and its numerical solution algorithm; in terms of theoretical properties, the symmetric Pareto EiCP is superior to the general EiCP. Under the non-negative cone constraint, the number of Pareto eigenvalues is finite, and the symmetric Pareto EiCP is equivalent to finding an equilibrium solution to a constrained optimization problem

$$\min_{x\in\triangle} \lambda(x) = \frac{x^\top Ax}{x^\top Bx}, \tag{1.3}$$

with respect to Rayleigh quotient function $\lambda(x)$, where the unit simplex $\triangle = \{x \in \mathbb{R}^n \mid x \geqslant 0,\ e_n^\top x = 1\}$ and $e_n \in \mathbb{R}^n$ is a vector of ones. That is, any Karush-Kuhn-Tucker point x in the above constraint optimization problem (1.3) is a solution of the symmetric Pareto EiCP [19], [23], [4], whose linear constraint $e_n^\top x = 1$ is to ensure $x \neq 0$. The paper [19] presents a projected steepest descent method to solve the symmetric Pareto EiCP, which uses the Armijo search condition to determine the step size. However, this strategy suffers from the problem of inexact search leading to too small step size, which results in slow convergence of the algorithm. Therefore, based on the projected steepest descent method, we combine the NCP function and the Rayleigh quotient gradient as the descent direction and use an exact linear search [4] rather than an inexact Armijo search to determine the step size, which improves the computational efficiency of the algorithms. Moreover, these algorithms are further extended to solve the Generalized Eigenvalue Complementarity Problem (GEiCP). Several numerical examples are used to validate the theoretical results and effectiveness of the algorithms, as well as to compare the computational efficiency of the algorithms proposed in the paper.

The structure of this paper is as follows. Section 2 focuses on the basic theory and properties of symmetric Pareto EiCP, as well as the descent algorithm framework for solving symmetric Pareto EiCP and its convergence proof. Section 3 introduces the symmetric Pareto GEiCP and its descent methods. Section 4 details the numerical experiments, and the last section summarizes some conclusions and recommendations for further work.

2. The symmetric Pareto EiCP

In this section, we concentrate on the symmetric Pareto EiCP, in which the mathematical formulation is given as: Find a scalar $\lambda \in \mathbb{R}$ and a nonzero vector $x \in \mathbb{R}^n$ such that

$$x \geqslant 0, \quad Ax - \lambda x \geqslant 0, \quad \langle x, Ax - \lambda x \rangle = 0, \tag{2.1}$$

where A is a given symmetric matrix. The symmetric Pareto EiCP (2.1) is equivalent to finding $\lambda \in \mathbb{R}$ such that

$$x \geqslant 0, \quad Ax - \lambda x \geqslant 0, \quad \langle x, Ax - \lambda x \rangle = 0, \quad \langle e_n, x \rangle = 1. \tag{2.2}$$

As stated in the introduction, we know that the symmetric Pareto EiCP (2.2) can be reduced to finding a stationary point of the constrained optimization problem

$$\min_{\substack{x \geqslant 0 \\ e_n^\top x = 1}} \lambda(x) = \frac{x^\top A x}{x^\top x}, \tag{2.3}$$

where the gradient of the Rayleigh quotient function $\lambda(x)$ is

$$\nabla \lambda(x) = \frac{2}{x^\top x}[A - \lambda(x) I]x. \tag{2.4}$$

The following lemma is the public condition that is helpful in the follow-up of this paper.

Lemma 2.1 ([19]). *For any $x \in \mathbb{R}^n \setminus \{0\}$, the following equalities hold:*

(1) $\lambda(\alpha x) = \lambda(x)$ *for all* $\alpha > 0$,
(2) $x^\top \nabla \lambda(x) = 0$.

Before proceeding further, let us introduce a merit function $\phi\colon \mathbb{R}^2 \to \mathbb{R}$, so-called an NCP function:

$$\phi(a,b) = 0 \Leftrightarrow a \geqslant 0,\ b \geqslant 0,\ ab = 0. \tag{2.5}$$

So far, a variety of NCP functions have been proposed, among which we focus on a well-known merit function, the Fischer-Burmeister NCP function, which is defined as

$$\phi(a,b) = a + b - \sqrt{a^2 + b^2} \quad \forall\,(a,b) \in \mathbb{R}^2. \tag{2.6}$$

With the above characterization of ϕ, the NCP function is equivalent to a system of nonsmooth equations:

$$\Phi(x,y) = \begin{pmatrix} \phi(x_1,y_1) \\ \phi(x_2,y_2) \\ \vdots \\ \phi(x_n,y_n) \end{pmatrix} = 0. \tag{2.7}$$

By combining the Rayleigh quotient gradient (2.4) and the Fischer-Burmeister NCP function (2.6), the basic properties of solutions to the symmetric Pareto EiCP (2.1) are given.

Theorem 2.1. *Let $x^* \geqslant 0$ be a nonzero vector and denote*

$$L^* = \{i \in I \mid x_i^* = 0\}, \quad F^* = \{i \in I \mid x_i^* > 0\},$$

where $I = \{1,2,\dots,n\}$. Then the following conclusions are equivalent:
(1) *x^* is a solution of* (2.1);
(2) *$\nabla_i\lambda(x^*) \geqslant 0$ for all $i \in L^*$ and $\nabla_i\lambda(x^*) = 0$ for all $i \in F^*$;*
(3) *$x^* = (x^* - \mu\nabla\lambda(x^*))_+$ for all $\mu > 0$;*
(4) *$\phi(x^*, \mu\nabla\lambda(x^*)) = 0$ for all $\mu > 0$.*

Proof. As can be seen from (2.1) and (2.4), nonzero vector x^* is the solution to problem (2.1) if and only if it satisfies

$$x^* \geqslant 0, \quad \nabla\lambda(x^*) \geqslant 0, \quad (x^*)^\top \nabla\lambda(x^*) = 0,$$

thus, proposition (1) is equivalent to proposition (2) by Lemma 2.1.

From proposition (2), it is clear that if $i \in L^*$, then $(x_i^* - \mu\nabla_i\lambda(x^*))_+ = 0$, and if $i \in F^*$, $(x_i^* - \mu\nabla_i\lambda(x^*))_+ = x_i^*$ holds, so we can obtain for all $\mu > 0$, $x^* = (x^* - \mu\nabla\lambda(x^*))_+$ and vice versa.

Another step in the proof is to show that proposition (2) is equivalent to proposition (4). In fact, if $\nabla_i\lambda(x^*) \geqslant 0$ for all $i \in L^*$, then $\phi(x_i^*, \mu\nabla_i\lambda(x^*)) = \mu\nabla_i\lambda(x^*) - \sqrt{(\mu\nabla_i\lambda(x^*))^2} = 0$, and if $\nabla_i\lambda(x^*) = 0$ for all $i \in F^*$, then $\phi(x_i^*, \mu\nabla_i\lambda(x^*)) = x_i^* - \sqrt{(x_i^*)^2} = 0$ holds. Conversely, by (2.5) and proposition (4), it is evident to observe that $x_i^* \geqslant 0, \nabla_i\lambda(x^*) \geqslant 0, (x_i^*)^\top\nabla_i\lambda(x^*) = 0$, which means that proposition (2) is established.

Summarizing what we have proved, we arrive at the conclusion that the four propositions above are equivalent. □

As mentioned in the introduction, the symmetric Pareto EiCP is equivalent to solving the equilibrium solution of a differentiable optimization problem. Inspired by the projected steepest descent method proposed in reference [19], combined with the reference [4], we establish a class of descent methods for solving symmetric Pareto EiCP. The formal steps of the descent algorithm framework are demonstrated below, and the symbol $\|\cdot\|$ without sub-index is also used to denote the Euclidean norm $\|\cdot\|_2$ in the following.

Framework 1 The Descent Algorithm of Symmetric Pareto EiCP

Input: Symmetric matrix $A \in \mathbb{R}^{n\times n}$;

Output: $x^* \geqslant 0$ such that x^* is a equilibrium solution of (2.3).

Initialize: Let $\varepsilon \in (0,1)$, $x^0 \geqslant 0$, and $e_n^\top x^0 = 1$; Repeat: $k = 0, 1, \ldots$;

Step 1. Compute

$$\nabla\lambda(x^k) = \frac{2}{(x^k)^\top x^k}[A - \lambda(x^k)I]x^k;$$

Step 2. Choose the descent direction d^k such that

$$\langle d^k, \nabla\lambda(x^k)\rangle \leqslant 0;$$

Step 3. Compute the step size $\mu^k \in [0,1]$ such that

$$x^k + \mu^k d^k \geqslant 0 \quad \text{and} \quad \lambda(x^k + \mu^k d^k) \leqslant \lambda(x^k);$$

Step 4. Update

$$v^{k+1} = x^k + \mu^k d^k, \quad x^{k+1} = \frac{v^{k+1}}{e_n^\top v^{k+1}};$$

Step 5. Set $k = k + 1$;

Until: Stopping criteria $\|d^k\| \leqslant 10^{-6}$ are met.

We can design the algorithm in the given algorithmic framework by changing the descent direction and step size. To begin, we utilize the projected steepest descent method (PSD) described in reference [19] to solve the symmetric Pareto EiCP, where the descent direction d^k and the step size μ^k by Armijo search are respectively denoted as follows:

$$d_i^k = \begin{cases} 0, & x_i^k = 0 \text{ and } \nabla_i \lambda(x^k) > 0, \\ -\nabla_i \lambda(x^k), & \text{otherwise}, \end{cases} \tag{2.8}$$

and $\mu^k = 1/2^{\tau_k}$, where τ_k is the minimum non-negative integer τ that satisfies

$$\begin{cases} x^k + \dfrac{1}{2^\tau} d^k \geqslant 0, \\ \lambda\Big(x^k + \dfrac{1}{2^\tau} d^k\Big) - \lambda(x^k) \leqslant \dfrac{\varepsilon}{2^\tau} \nabla \lambda(x^k)^\top d^k. \end{cases} \tag{2.9}$$

If $d^k \neq 0$, then we can immediately draw the following conclusions:

(a) $\nabla \lambda(x^k)^\top d^k = -(d^k)^\top d^k < 0$;
(b) $(x^k)^\top d^k = -(x^k)^\top \nabla \lambda(x^k) = 0$;
(c) $(x^k)^\top v^{k+1} = (x^k)^\top (x^k) > 0$;
(d) $v^{k+1} \neq 0$.

It is worth mentioning that a similar convergence theorem for the projected steepest descent method has been proved in [19] and will not be reproduced here.

Through the clarity of exposition of the PSD method, other line search strategies and descent directions d^k (such that $\nabla \lambda(x^k)^\top d^k < 0$) can be utilized. Therefore, in what follows, we propose two different strategies. The first is that we suggest a descent direction based on the NCP function, known as the NCP-based descent method (NCPD), which is given as

$$d_i^k = -\phi(x_i^k, \nabla_i \lambda(x^k)), \quad i = 1, 2, \ldots, n. \tag{2.10}$$

The other strategy is to combine (2.8) with (2.10), whereby the spectral block descent method (SBD) is obtained

$$d_i^k = \begin{cases} -x_i^k & \text{if } x_i^k \leqslant \beta \nabla_i \lambda(x^k), \\ -\phi(x_i^k, \nabla_i \lambda(x^k)) & \text{if } \beta \nabla_i \lambda(x^k) < x_i^k < \nabla_i \lambda(x^k), \\ -\nabla_i \lambda(x^k) & \text{if } x_i^k \geqslant \nabla_i \lambda(x^k), \end{cases} \tag{2.11}$$

where β denotes a given positive number. For the $d^k \neq 0$ generated by Algorithm NCPD and Algorithm SBD respectively, we have the following results.

Lemma 2.2. *For the sequences* $\{x^k\}$ *generated by Algorithm* NCPD *and Algorithm* SBD, *respectively, where* $x^k \geqslant 0$, *and* $\nabla\lambda(x^k)$ *is defined by* (2.4), *we have*

(a) $\nabla\lambda(x^k)^\top d^k \leqslant -\eta\|d^k\|^2$, $\eta > 0$;
(b) $x^k + \mu d^k \geqslant 0$ *for all* $\mu \in [0,1]$;
(c) $x^k + \mu d^k \neq 0$ *for all* $\mu \in \mathbb{R}$.

P r o o f. *Part 1.* Our first goal is to show that the conclusions hold under the NCPD algorithm with d_i^k being defined as (2.10).

(a) Consider the component of $\nabla\lambda(x^k)^\top d^k$, assume there exists such $\eta > 0$ that $\nabla_i\lambda(x^k)d_i^k \leqslant -\eta(d_i^k)^2$. When $d_i^k = 0$, assertion (a) is obviously valid.

Suppose now that $d_i^k \neq 0$.

If $d_i^k < 0$, then $\nabla_i\lambda(x^k) \geqslant -\eta d_i^k$. According to formula (2.6), it follows that

$$\nabla_i\lambda(x^k) \geqslant \eta\Big(x_i^k + \nabla_i\lambda(x^k) - \sqrt{(x_i^k)^2 + \nabla_i^2\lambda(x^k)}\Big),$$

which implies

$$\eta \leqslant \frac{\nabla_i\lambda(x^k)}{x_i^k + \nabla_i\lambda(x^k) - \sqrt{(x_i^k)^2 + \nabla_i^2\lambda(x^k)}}. \tag{2.12}$$

Conversely, if $d_i^k > 0$, then $\nabla_i\lambda(x^k) \leqslant -\eta d_i^k$, formula (2.6) yields

$$\nabla_i\lambda(x^k) \leqslant \eta\Big(x_i^k + \nabla_i\lambda(x^k) - \sqrt{(x_i^k)^2 + \nabla_i^2\lambda(x^k)}\Big),$$

which obtains

$$\eta \leqslant \frac{\nabla_i\lambda(x^k)}{x_i^k + \nabla_i\lambda(x^k) - \sqrt{(x_i^k)^2 + \nabla_i^2\lambda(x^k)}}. \tag{2.13}$$

Combining (2.12) with (2.13), we have

$$0 < \eta \leqslant \frac{\nabla_i\lambda(x^k)}{x_i^k + \nabla_i\lambda(x^k) - \sqrt{(x_i^k)^2 + \nabla_i^2\lambda(x^k)}}. \tag{2.14}$$

Thus, there exists $\eta > 0$ such that assertion (a) holds.

(b) The assertion is obviously implied by $x^k \geqslant 0$ and $\mu \in [0,1]$, that is,

$$\begin{aligned} x^k + \mu d^k &= (1-\mu)x^k + \mu\Big(\sqrt{(x^k)^2 + (\nabla\lambda(x^k))^2} - \nabla\lambda(x^k)\Big) \\ &\geqslant \mu\Big(\sqrt{(x^k)^2 + (\nabla\lambda(x^k))^2} - \nabla\lambda(x^k)\Big) \geqslant 0. \end{aligned}$$

(c) Let us assume the contrary, i.e., there exists $\widehat{\mu} \in \mathbb{R}$ such that $x^k + \widehat{\mu} d^k = 0$. Because $x^k \in \{x \in \mathbb{R}^n \mid x \geqslant 0, e_n^\top x = 1\}$ we know that $x^k \neq 0$, and, in turn, that $\widehat{\mu} \neq 0$ and $d^k = -x^k/\widehat{\mu} \neq 0$. Therefore, assertion (a) implies that

$$\lambda(x^k + \mu d^k) = \lambda\Big(\Big(1 - \frac{\mu}{\widehat{\mu}}\Big)x^k\Big) < \lambda(x^k)$$

is valid for some $0 < \mu < |\widehat{\mu}|$. Since $(1 - \mu/\widehat{\mu}) \notin \{0, 1\}$, this contradicts Lemma 2.1. Hence, assertion (c) is valid.

Part 2. The proof of the second part of this lemma proceeds in a similar manner, where d_i^k is generated by (2.11) of the SBD algorithm.

(a) We first show that if $\beta \nabla_i \lambda(x^k) < x_i^k < \nabla_i \lambda(x^k)$, then $d_i^k = -\phi(x_i^k, \nabla_i \lambda(x^k))$. From the fact that $x_i^k \geqslant 0$, we have

$$\beta < \frac{x_i^k}{\nabla_i \lambda(x^k)} < 1. \tag{2.15}$$

Suppose that there exists such $\widehat{\eta} > 0$ that $\nabla_i \lambda(x^k) d_i^k \leqslant -\widehat{\eta}(d_i^k)^2$. By formula (2.6), it is easy to show that $\nabla_i \lambda(x^k) \geqslant \widehat{\eta}\big(x_i^k + \nabla_i \lambda(x^k) - \sqrt{(x_i^k)^2 + \nabla_i^2 \lambda(x^k)}\big)$, then (2.15) yields

$$0 < \widehat{\eta} < 1 + \frac{\sqrt{2}}{2}. \tag{2.16}$$

Hence, assertion (a) is proved in this situation. For the remaining indices, we have

$$\nabla_i \lambda(x^k) d_i^k = -\nabla_i \lambda(x^k) x_i^k \leqslant -\frac{1}{\beta}(d_i^k)^2 \quad \text{if } x_i^k \leqslant \beta \nabla_i \lambda(x^k), \tag{2.17}$$

$$\nabla_i \lambda(x^k) d_i^k = -(d_i^k)^2 \quad \text{if } x_i^k \geqslant \nabla_i \lambda(x^k). \tag{2.18}$$

On account of (2.16), (2.17), and (2.18), assertion (a), that is $\nabla \lambda(x^k)^\top d^k \leqslant -\eta \|d^k\|^2$, follows with $\eta = \max\{1/\beta, \widehat{\eta}, 1\}$.

Assertion (b) is obviously inferred by $x^k \geqslant 0$ and the definition of d^k. In addition, the proof of assertion (c) is quite similar to the previous assertion (c) of part 1 and so is omitted.

Summarizing Part 1 and Part 2, the proof of this lemma is now completed. □

Lemma 2.2 indicates that the search directions defined by Algorithms NCPD and SBD are the descent directions. Moreover, when the step size $\mu^k \in [0, 1]$, the non-negative of the iteration vector $\{x^k\}$ can be guaranteed, so there is no need to search for the step size. Based on the above findings, we can use the following method (exact linear search) to select the optimal step size μ_k to replace the Armijo step size.

Let μ_k be a solution of the optimization problem

$$\min_{0\leqslant\mu\leqslant 1} \varphi(\mu) := \lambda(x^k + \mu d^k). \tag{2.19}$$

Since $\varphi(\mu)$ is continuously differentiable, to find a solution of (2.19), we need to consider zeros of $\varphi'(\mu)$ and define the following parameters a_0, a_1, and a_2 as

$$a_0 = a_0(d^k, x^k), a_1 = a_1(d^k, x^k), a_2 = a_2(d^k, x^k),$$

where

$$\begin{aligned} a_0(d,x) &:= (d^\top Ax)(x^\top x) - (d^\top x)(x^\top Ax), \\ a_1(d,x) &:= (d^\top Ad)(x^\top x) - (d^\top d)(x^\top Ax), \\ a_2(d,x) &:= (d^\top Ad)(x^\top d) - (d^\top d)(x^\top Ad). \end{aligned}$$

Each solution of $\varphi'(\mu) = 0$ is a root of the quadratic equation $a_0 + a_1\mu + a_2\mu^2 = 0$, and vice versa.

Theorem 2.2 ([4]). *If the quadratic equation $a_0 + a_1\mu + a_2\mu^2 = 0$ has two real roots μ_1 and μ_2 (possibly equal) with $\mu_1 \leqslant \mu_2$, then the step size μ_k can be determined by*

$$\mu^k = \begin{cases} 1 & \textit{if there is no solution in } [0,1], \\ \arg\min\{\varphi(\mu_2), \varphi(1)\} & \textit{if there is only } \mu_2 \in [0,1], \\ \arg\min\{\varphi(\mu_1), \varphi(1)\} & \textit{otherwise.} \end{cases} \tag{2.20}$$

Therefore, we can present the convergence theorem of Algorithm NCPD and Algorithm SBD.

Theorem 2.3. *Each accumulation point x^* of the sequence $\{x^k\}$ generated by Algorithm NCPD is a solution of the symmetric Pareto EiCP* (2.2).

Proof. First notice that the direction d^k (2.10) is a descent direction. From Lemma 2.2, we know that $v^{k+1} \neq 0$.

By Lemma 2.1, the renormalization preserves the value of the objective function

$$\lambda(x^{k+1}) = \lambda\Big(\frac{v^{k+1}}{e_n^\top v^{k+1}}\Big) = \lambda(v^{k+1}),$$

as well as the constraint $x^k \geqslant 0$. Therefore, the sequence $\{x^k\}$ is well-defined and belongs to the compact set $\triangle = \{x \in \mathbb{R}^n \mid x \geqslant 0, e_n^\top x = 1\}$. Then there exists a convergent subsequence $\{x^k\}$ converging to x^*. According to the definition of d^k (see (2.10)) and formula (2.6), we can infer that

$$\begin{aligned}\|d^k\|_2^2 &= \|-\phi(x^k, \nabla\lambda(x^k))\|_2^2 \\ &= |\phi(x_1^k, \nabla_1\lambda(x^k))|^2 + |\phi(x_2^k, \nabla_2\lambda(x^k))|^2 + \ldots + |\phi(x_n^k, \nabla_n\lambda(x^k))|^2 \\ &\leqslant \big(\sqrt{2}+1\big)^2(\|x^k\|_2^2 + \|\nabla\lambda(x^k)\|_2^2) \leqslant 2\big(\sqrt{2}+1\big)^2 \max\{\|x^k\|_2^2, \|\nabla\lambda(x^k)\|_2^2\}.\end{aligned}$$

Due to $x^k \in \triangle$, it follows that $\|x^k\|_2 \leqslant \|x^k\|_1 = 1$. Then

$$\|d^k\|_2 \leqslant \big(2+\sqrt{2}\big)\max\{\|x^k\|_2, \|\nabla\lambda(x^k)\|_2\} \leqslant M, \tag{2.21}$$

where $M = \big(2+\sqrt{2}\big)(\max\{\|\nabla\lambda(x^k)\|_2 \mid x \in \triangle\} + 1)$. Hence, d^k is bounded.

Next, we have to prove that $\lim\limits_{x\to\infty} d^k = 0$. There exists a compact set

$$\mathcal{C} = \{x \in \mathbb{R}^n \mid 0 < \|x\|_2 \leqslant M + 1\}.$$

Obviously, $x^k + \mu d^k \in \mathcal{C}$ for all $\mu \in [0,1]$. Since $\lambda(x)$ is twice continuously differentiable on compact set $\mathcal{C}$ and $0 \notin \mathcal{C}$,

$$\theta = \max\{\|\nabla^2\lambda(x)\|_2 \mid x \in \mathcal{C}\} + 1$$

is well defined. Therefore, Taylor's formula and Lemma 2.2 imply

$$\begin{aligned}\lambda(x^k + \mu d^k) &\leqslant \lambda(x^k) + \mu\nabla\lambda(x^k)^\top d^k + \frac{1}{2}\mu^2\theta\|d^k\|_2^2 \\ &\leqslant \lambda(x^k) + \mu\Big(-\eta + \frac{1}{2}\mu\theta\Big)\|d^k\|_2^2,\end{aligned} \tag{2.22}$$

where $\mu \in [0,1]$. Let $\mu_{\min} = \min\{\eta/\theta, 1\} \subset [0,1]$. We have $-\eta + \frac{1}{2}\mu_{\min}\theta \leqslant -\frac{1}{2}\eta$. From (2.22) and the exact linear search, it can be derived

$$\lambda(x^{k+1}) = \lambda(v^{k+1}) = \lambda(x^k + \mu_k d^k) \leqslant \lambda(x^k) - \frac{1}{2}\eta\mu_{\min}\|d^k\|_2^2. \tag{2.23}$$

By the fact that $\lambda(x)$ is continuous on the compact set $\mathcal{C}$ and $x^k \in \mathcal{C}$, it follows that the sequence $\{\lambda(x^k)\}$ is bounded below. Then (2.23) yields

$$\lim_{k\to\infty} d^k = 0.$$

Thus, we arrive at the conclusion that x^* is a stationary point of the optimization problem (2.3), and from Theorem 2.1 it can be seen that x^* is a solution of the symmetric Pareto EiCP (2.2). □

Theorem 2.4. *Each accumulation point x^* of the sequence $\{x^k\}$ generated by Algorithm* SBD *is a solution of the symmetric Pareto* EiCP (2.2).

P r o o f. The only difference between Theorem 2.3 and Theorem 2.4 is the selection of d^k. It is easy to verify that $\|d^k\|_2$ in the SBD algorithm has a similar result as Theorem 2.3. The remainder of the argument is quite similar to that given earlier for the convergence theorem and so is omitted here. □

3. The symmetric Pareto GEiCP

In the previous section of this paper, we introduced three algorithms by choosing different descent directions and step sizes, as well as how to prove the convergence of the proposed algorithms. The main contributions of this section are that the theoretical foundations and numerical solution methods for symmetric Pareto EiCP presented in the previous part are extended to a symmetric Pareto Generalized Eigenvalue Complementarity Problem (GEiCP) based on the special structure and properties of symmetric matrices.

Definition 3.1. For given matrices $A, B \in \mathbb{R}^{n\times n}$, let $\lambda \in \mathbb{R}$ be a scalar and $x \in \mathbb{R}^n$ a nonzero vector satisfying $y = (A - \lambda B)x$ and

$$y_J \geqslant 0, \quad y_{J^c} = 0, \quad x_J \geqslant 0, \quad \langle y_J, x_J\rangle = 0, \tag{3.1}$$

where $J \subseteq I = \{1, 2, \ldots, n\}$ is given, and $J^c = I \setminus J$. Problem (3.1) is called the Pareto Generalized Eigenvalue Complementarity Problem (GEiCP). For any solution (λ, x), the value λ and x are respectively said to be a generalized complementarity eigenvalue and an associated generalized complementarity eigenvector for the given pair (A, B).

R e m a r k 3.1 ([19]). (1) There may be infinitely many real numbers λ satisfying (3.1) for the special matrix pair (A, B). For example:

$$A = \begin{pmatrix} 1 & 1 & 0\\ 1 & 0 & 0\\ 0 & 0 & 1\end{pmatrix}, \quad B = \begin{pmatrix} 1 & 0 & 0\\ 0 & 0 & 0\\ 0 & 0 & 1\end{pmatrix}, \quad J = \{1, 2\}.$$

(2) If $B \in \mathbb{R}^{n\times n}$ is a symmetric positive definite matrix, GEiCP has at most $(2n - |J|)2^{|J|-1}$ distinct generalized complementarity eigenvalues.

(3) When $J \in \{1, 2, \ldots, n\}$, we have $(2n - |J|)2^{|J|-1} = n2^{n-1}$.

The symmetric Pareto GEiCP is to find $\lambda \geqslant 0$ and $x \in \mathbb{R}^n$ such that $y = (A - \lambda B)x$ and

$$y_J \geqslant 0, \quad y_{J^c} = 0, \quad x_J \geqslant 0, \quad \langle y_J, x_J \rangle = 0, \quad \|x\| = 1, \tag{3.2}$$

where $A, B \in \mathbb{R}^{n \times n}$ are given symmetric matrices, B is a symmetric positive definite.

It is obvious from Remarks (2) and (3) that the number of generalized complementary eigenvalues for symmetric Pareto GEiCP is finite. Due to x not always being non-negative (only x_J is non-negative), the condition $x \neq 0$ cannot be substituted by $e_n^\top x = 1$. Without loss of generality, the solution of the symmetric Pareto GEiCP is constrained to find with the range of $\|x\| = 1$. Furthermore, the following conclusions can be drawn:

Once again the symmetric Pareto GEiCP (3.2) can be reduced to a constrained optimization problem in which the goal is to find a fixed point. That is, every equilibrium solution $x \in \mathbb{R}^n$ of the constrained optimization problem

$$\min_{\substack{x_J \geqslant 0 \\ \|x\|=1}} \lambda(x) = \frac{x^\top A x}{x^\top B x} \tag{3.3}$$

is a solution of the symmetric Pareto GEiCP (3.2). The gradient of the generalized Rayleigh quotient function $\lambda(x)$ is defined as

$$\nabla \lambda(x) = \frac{2}{x^\top B x}[A - \lambda(x) B]x. \tag{3.4}$$

For any $x \in \mathbb{R}^n \setminus \{0\}$, the generalized Rayleigh quotient retains the two fundamental properties of Lemma 2.1.

Theorem 2.1 can then be extended to the symmetric Pareto GEiCP (3.2). Combining the gradient function (3.4) with the Fischer-Burmeister NCP-function (2.6), we get the following basic properties.

Theorem 3.1. *Let $x^* \geqslant 0$ be a nonzero vector and denote*

$$L^* = \{i \in J \mid x_i^* = 0\}, \quad F^* = \{i \in J \mid x_i^* > 0\}.$$

Then the following conclusions are equivalent:

(1) *x^* is a solution of the symmetric Pareto* GEiCP (3.2);
(2) *$\nabla_i \lambda(x^*) \geqslant 0$ for all $i \in L^*$, and $\nabla_i \lambda(x^*) = 0$ for all $i \in F^*$;*
(3) *$x_J^* = (x_J^* - \mu \nabla_J \lambda(x^*))_+$ for all $\mu > 0$;*
(4) *$\phi(x_i^*, \mu \nabla_i \lambda(x^*)) = 0$ for all $\mu > 0$, $i \in J$.*

P r o o f. By (3.2) and (3.4), nonzero vector x^* is a solution to problem (3.2) if and only if it satisfies

$$\nabla_J \lambda(x^*) \geqslant 0, \quad \nabla_{J^c} \lambda(x^*) = 0, \quad x^*_J \geqslant 0, \quad \langle \nabla_J \lambda(x^*), x^*_J \rangle = 0.$$

The remainder of the proof is analogous to that of Theorem 2.1 and will not be given here. □

Next, we propose the descent algorithm framework 2, which is applied to the symmetric Pareto GEiCP.

Framework 2 The Descent Algorithm of Symmetric Pareto GEiCP

Input: Symmetric matrix A and symmetric positive definite matrix B.

Output: $x^* \geqslant 0$ such that x^* is a equilibrium solution of (3.3).

Initialize: Let $\varepsilon \in (0,1)$, $x^0 \geqslant 0$ and $\|x^0\| = 1$; Repeat: $k = 0, 1, \ldots$,

Step 1. Compute

$$\nabla \lambda(x^k) = \frac{2}{(x^k)^\top B x^k} [A - \lambda(x^k) B] x^k;$$

Step 2. Choose the descent direction d^k such that

$$\langle d^k, \nabla \lambda(x^k) \rangle \leqslant 0;$$

Step 3. Compute a step size $\mu^k \in [0,1]$ such that

$$x^k_J + \mu^k d^k_J \geqslant 0 \quad \text{and} \quad \lambda(x^k + \mu^k d^k) \leqslant \lambda(x^k);$$

Step 4. Update

$$v^{k+1} = x^k + \mu^k d^k, \quad x^{k+1} = \frac{v^{k+1}}{\|v^{k+1}\|};$$

Step 5. Set $k = k + 1$;

Until: Stopping criteria $\|d^k\| \leqslant 10^{-6}$ are met.

Under the above algorithm framework, we can still select different descent directions and step sizes, as we did in the previous part, to obtain different algorithms for calculating this problem (3.3). Firstly, we solve the symmetric Pareto GEiCP using the projected steepest descent method (PSD) presented in reference [19], for short (GPSD). Let

$$d^k_i = \begin{cases} 0, & i \in J,\ x^k_i = 0 \text{ and } \nabla_i \lambda(x^k) > 0, \\ -\nabla_i \lambda(x^k), & \text{otherwise}, \end{cases} \tag{3.5}$$

and the Armijo step size $\mu^k = 1/2^{\tau_k}$, where τ_k is the minimum non-negative integer τ that satisfies

$$\begin{cases} x_J^k + \dfrac{1}{2^\tau} d_J^k \geqslant 0, \\ \lambda\Big(x^k + \dfrac{1}{2^\tau} d^k\Big) - \lambda(x^k) \leqslant \dfrac{\varepsilon}{2^\tau} \nabla\lambda(x^k)^\top d^k. \end{cases} \tag{3.6}$$

Our results from Algorithm GPSD are nearly identical to those established in Algorithm PSD, so we will not repeat them here.

In what follows, we determine the descent direction by utilizing the NCP function (2.6) and formula (3.5), which obtains the following spectral block descent algorithm for computing symmetric Pareto GEiCP (GSBD), given as

$$d_i^k = \begin{cases} -\phi(x_i^k, \nabla_i \lambda(x^k)), & i \in J, \\ -\nabla_i \lambda(x^k), & i \notin J. \end{cases} \tag{3.7}$$

If $d^k \neq 0$, as an immediate consequence of the iterative step, we now have

(1) $\nabla\lambda(x^k)^\top d^k \leqslant -\eta \|d^k\|^2$, $\eta > 0$;
(2) $x_J^k + \mu d_J^k \geqslant 0$ for all $\mu \in [0,1]$;
(3) $x^k + \mu d^k \neq 0$ for all $\mu \in \mathbb{R}$.

Instead of the inexact Armijo search, we use the exact linear search, as described in the previous section, to determine the optimal step size μ^k for the GSBD algorithm. Let μ_k be a solution of the optimization problem $\min\limits_{0\leqslant\mu\leqslant 1} \varphi(\mu) := \lambda(x^k + \mu d^k)$, and the values a_0, a_1, a_2 are defined by $a_0 = a_0(d^k, x^k)$, $a_1 = a_1(d^k, x^k)$, $a_2 = a_2(d^k, x^k)$, where

$$\begin{aligned} a_0(d,x) &:= (d^\top Ax)(x^\top Bx) - (d^\top Bx)(x^\top Ax), \\ a_1(d,x) &:= (d^\top Ad)(x^\top Bx) - (d^\top Bd)(x^\top Ax), \\ a_2(d,x) &:= (d^\top Ad)(x^\top Bd) - (d^\top Bd)(x^\top Ad). \end{aligned}$$

We know that each solution of $\varphi'(\mu) = 0$ is a root of the quadratic equation $a_0 + a_1\mu + a_2\mu^2 = 0$. Then the step size μ_k can be determined by Theorem 2.2.

Based on the above discussion, we next establish the main convergence result for Algorithm GSBD. Moreover, the proof uses the same methodology as Theorem 2.3 and Theorem 2.4.

Theorem 3.2. *Each accumulation point x^* of the sequence $\{x^k\}$ generated by Algorithm* GSBD *is a solution of the symmetric Pareto* GEiCP (3.2).

4. Numerical experiments

In this section, we present the results of some numerical experiments aimed at examining the performance of the presented descent algorithms, i.e., PSD, NCPD, and SBD, in terms of the elapsed CPU time in seconds (denoted by "CPU"). All the tests are performed using MATLAB 7.10, which has a machine precision of around 10^{-16}. In all cases, we set the stopping criterion for each algorithm as

$$\|d^k\| \leqslant 10^{-6}.$$

We also check the complementarity condition of x^k by the residual

$$\operatorname{Res}(x^k) = \|\min(x^k, \nabla\lambda(x^k))\|.$$

Firstly, we employ a small problem to test and verify the theoretical results as well as the effectiveness of the algorithms proposed.

Example 4.1. Consider solving a low-dimensional symmetric matrix as follows:

$$A = \begin{pmatrix} 4 & -7 & 0 & 0 \\ -7 & -2 & 6 & 0 \\ 0 & 6 & 2 & -1 \\ 0 & 0 & -1 & 0 \end{pmatrix} \quad \text{and} \quad x_0 = \begin{pmatrix} 1 \\ 0 \\ 0 \\ 0 \end{pmatrix},$$

where x_0 is the iterative initial vector. By using Algorithms PSD, NCPD, and SBD, respectively, the numerical results of these algorithms are

$$\lambda(x^*) = -6.6158, \quad x^* = \begin{pmatrix} 0.3974 \\ 0.6026 \\ 0 \\ 0 \end{pmatrix}, \quad Ax^* - \lambda(x^*)x^* = \begin{pmatrix} 0 \\ 0 \\ 3.6158 \\ 0 \end{pmatrix}.$$

It is worth mentioning that $\lambda(x^*)$ and x^* satisfy the symmetric Pareto EiCP (2.1), which means that $\lambda(x^*)$ and x^* are the Pareto eigenvalue and an associated Pareto eigenvector of this problem, respectively. The performance profiles given by the Algorithms PSD, NCPD, and SBD are shown in Figure 1. Algorithms NCPD and SBD have better convergence performance than Algorithm PSD. The main reason is that Algorithm PSD employs inexact Armijo linear search step length, as it gets closer to the convergence solution, the amount of decrease in step size becomes smaller, resulting in slow convergence rate of the algorithm.

Example 4.1 shows the effectiveness of the methods presented in the paper. Following that, we validate and compare the numerical performance of the algorithms proposed in this paper to the PSD method by using random test problems.

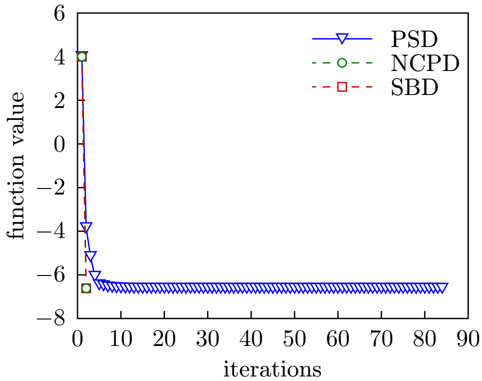

Figure 1. Comparing PSD, NCPD, and SBD based on performance profiles of the iterations.

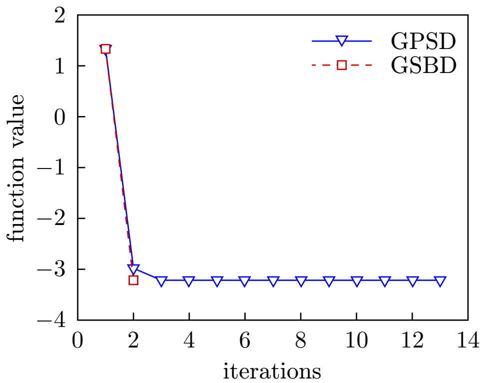

Figure 2. Comparing GPSD and GSBD based on performance profiles of the iterations.

Example 4.2. In this example, the entries of B generated by MATLAB are random numbers from the uniform distribution on the interval $[-1,1]$, and set

$$A = B + B^{\top}.$$

We use $x^0 = \frac{1}{n}(1,1,\dots,1) \in \mathbb{R}^n$ as the initial guess, and each cell in the following table gives the CPU time taken by Algorithms PSD, NCPD, and SBD for solving the symmetric Pareto EiCP with various sizes. The symbol "$*$" denotes that the required CPU time exceeds 500 seconds.

Table 1 summarizes the numerical performance of Example 4.2, which shows that Algorithms NCPD and SBD quickly converge to the final solution for this problem, while the performance of Algorithm PSD in practical calculations worsens as the matrix dimension increases and eventually suffers from the problem of convergence stagnation. Although it is theoretically proven that the step size in the PSD method declines continuously as the iteration progresses, in practice, the amount of decline for step size becomes very small as it gets closer to the final solution for this problem, which may eventually lead to the required results not being obtained within the calculation time available or convergence stagnation. Following our improvement, which uses the exact linear search obtained by solving a quadratic equation with one variable to determine the step length and combine the negative gradient direction with the NCP function to obtain new descent directions d^k, as shown in (2.10) and (2.11), that is, Algorithms NCPD and SBD, it not only reduces running time but also significantly improves the convergence accuracy.

n	Algorithm	CPU	$\lambda(x^k)$	$\mathrm{Res}(x^k)$	$\|d^k\|$
$n=5$	PSD	0.0023	−2.3652	2.3871e−07	2.3871e−07
	NCPD	0.0015	−2.3652	8.4090e−07	8.4089e−07
	SBD	0.0041	−2.3652	9.0759e−07	9.0759e−07
$n=10$	PSD	500*	−1.2000*	4.1275*	10.5984*
	NCPD	0.0070	−2.2111	9.4151e−07	9.4151e−07
	SBD	0.0034	−2.2111	5.3827e−07	5.3827e−07
$n=20$	PSD	500*	−0.5233*	9.4340*	26.9916*
	NCPD	0.0126	−3.2077	8.9483e−07	8.9484e−07
	SBD	0.0146	−3.2077	2.3514e−08	2.3514e−08
$n=50$	PSD	500*	−1.6133*	40.6806*	79.6440*
	NCPD	0.1438	−7.2961	9.9894e−07	9.9894e−07
	SBD	0.1472	−7.2961	9.8814e−07	9.8814e−07
$n=100$	PSD	500*	−4.3991*	49.5466*	103.7764*
	NCPD	0.6881	−11.0830	9.9843e−07	9.9842e−07
	SBD	0.7512	−11.0830	9.9564e−07	9.9564e−07
$n=500$	PSD	500*	−11.0320*	353.4802*	683.6907*
	NCPD	21.9640	−25.8153	9.9764e−07	9.9763e−07
	SBD	27.1762	−25.8153	9.9969e−07	9.9969e−07
$n=1000$	PSD	500*	−15.3659*	683.4686*	1.3277e+03*
	NCPD	178.6844	−35.7000	9.9866e−07	9.9865e−07
	SBD	231.3704	−35.7000	1.0000e−06	1.0000e−06

Table 1. CPU times of algorithms when solving random test problems.

The performance of Algorithms GPSD and GSBD for solving the symmetric Pareto GEiCP (3.2) with B being a symmetric positive definite matrix is reported in the following section. We check the complementarity condition of x^k by the residual

$$\mathrm{Res}(x^k) = \|\min(x^k_J, \nabla_J \lambda(x^k))\|.$$

As with the test problems shown above, we begin with a small problem to verify the validity of Algorithms GPSD and GSBD.

Without loss of generality, the following test problems are adapted from Examples 4.1 and 4.2.

Example 4.3. In this example, we set $J = \{1, 3, 4\}$,

$$A = \begin{pmatrix} 4 & -7 & 0 & 0 \\ -7 & -2 & 6 & 0 \\ 0 & 6 & 2 & -1 \\ 0 & 0 & -1 & 0 \end{pmatrix}, \quad B = \begin{pmatrix} 3 & -1 & 0 & 0 \\ -1 & 3 & -1 & 0 \\ 0 & -1 & 3 & -1 \\ 0 & 0 & -1 & 3 \end{pmatrix}, \quad x_0 = \begin{pmatrix} 1 \\ 0 \\ 0 \\ 0 \end{pmatrix}.$$

By using Algorithms GPSD and GSBD, the numerical results of these algorithms are

$$\lambda(x^*) = -3.2157, \quad x^* = \begin{pmatrix} 0.5993 \\ 0.8006 \\ 0 \\ 0 \end{pmatrix}, \quad Ax^* - \lambda(x^*)Bx^* = \begin{pmatrix} 0 \\ 0 \\ 2.2290 \\ 0 \end{pmatrix},$$

which means that $\lambda(x^*)$ and x^* are the Pareto generalized complementarity eigenvalue and an associated Pareto generalized complementarity eigenvector of this problem, respectively. Figure 2 depicts the performance profiles by adopting Algorithms GPSD and GSBD, which reveals that Algorithm GSBD converges faster than Algorithm GPSD because the former uses an exact linear search to determine the step size, whereas the latter utilizes an inexact Armijo search strategy, which leads to small step sizes due to inexact search, resulting in very slow convergence of the algorithm.

Example 4.4. In this example, the entries of C generated by MATLAB are random numbers from the uniform distribution on the interval $[-1, 1]$, and set

$$A = C + C^\top, \quad B = \text{tridiag}\{-1, 3, -1\}.$$

The index set J is composed of all the odd numbers selected from $I = \{1, 2, \dots, n\}$. We use $x^0 = (1, 0, \dots, 0) \in \mathbb{R}^n$ as the initial guess, and each cell in the following table gives the CPU time taken by Algorithm GPSD and Algorithm GSBD for solving the symmetric Pareto GEiCP with various sizes. The symbol "$*$" denotes that required CPU time exceeds 100 seconds.

The results in Table 2 indicate that Algorithm GSBD is preferable to Algorithm GPSD in terms of numerical performance. Despite the theoretical convergence for Algorithm GPSD, it causes complicated computation indeed and only works well for some low-order matrices. It is noteworthy that as the matrix dimension increases, our method requires more CPU time to obtain the approximate solution, especially for the large-scale test problem. As a result, we anticipate investigating the algorithm further to improve the numerical performance of the large-scale Pareto Eigenvalue Complementarity Problem.

n	Algorithm	CPU	$\lambda(x^k)$	$\mathrm{Res}(x^k)$	$\|d^k\|$
$n = 5$	GPSD	0.0018	-1.8199	3.7219e$-$07	7.7745e$-$07
	GSBD	0.0044	-1.8199	3.2163e$-$07	5.3590e$-$07
$n = 10$	GPSD	0.0054	-2.2381	5.9527e$-$07	9.3455e$-$07
	GSBD	0.0070	-2.2381	4.4566e$-$07	5.8994e$-$07
$n = 20$	GPSD	100*	-0.9230*	1.0492*	1.5200*
	GSBD	0.0172	-2.9342	1.0552e$-$06	9.8404e$-$07
$n = 50$	GPSD	100*	-2.3829*	2.3281*	4.1696*
	GSBD	0.0295	-5.6935	4.9139e$-$07	9.2280e$-$07
$n = 100$	GPSD	100*	-1.5765*	5.5084*	4.5919*
	GSBD	0.0398	-6.5039	7.0040e$-$07	8.5879e$-$07
$n = 500$	GPSD	100*	-2.3644*	26.8406*	14.6432*
	GSBD	1.1752	-16.6567	5.8668e$-$07	9.6775e$-$07
$n = 1000$	GPSD	100*	-2.3993*	48.7655*	20.6335*
	GSBD	13.9229	-24.1042	6.2489e$-$07	9.7899e$-$07

Table 2. CPU times of Algorithms when solving random test problems.

Example 4.5. In this example, we focus on the application of our algorithm, which applies the GSBD Algorithm to solve a practical problem, where $J = \{1, 2, \ldots, n\}$. Frictional vibration, a phenomenon to be avoided in engineering, is often caused by unilateral frictional contact. After a unilateral friction contact system is discretized through the finite element method, a complementary problem will be formed, thus the theoretical analysis of this complementary problem has an application value in reality [26]. In a physical sense, its complementary eigenvalues and corresponding eigenvectors can properly reflect how the instability occurs in frictional contact.

Figure 3 shows that the object is ready for translational motion in a plane with friction coefficient δ, which is a representative of a typical unilateral friction contact model. According to the element model proposed in [17], the unilateral friction contact system presented in Figure 3 is discretized by the finite element method, and the two-node element model used is shown in Figure 4, in which we assume that at the quasi equilibrium state, both nodes 1 and 2 are in impending slip to the left. In this state, when a node has a slide speed greater than 0, the force it bears will remain a constant value (the maximum static friction force) and will not vary with the speed change, which means that the change rate of force at this node will equal to 0. The eigenproblem is governed by

$$(\widetilde{K} + \widetilde{K}_\delta)v = r, \tag{4.1}$$

$$0 \leqslant v \perp r \geqslant 0, \tag{4.2}$$

where υ and r, respectively, stand for the sliding velocity and the change rate of force, and the friction coefficient $\delta \geqslant 0$ at that transition is also an unknown. The sum $\widetilde{K} + \widetilde{K}_\delta$ is the element stiffness matrix, in which $\widetilde{K}_\delta = \delta I$ and $\widetilde{K}$ is determined by the material properties of the element stiffness matrix, defined as

$$\widetilde{K} = \begin{pmatrix} 4\varrho + \dfrac{2(1-\sigma)}{\varrho} & -4\varrho + \dfrac{1-\sigma}{\varrho} \\ -4\varrho + \dfrac{1-\sigma}{\varrho} & 4\varrho + \dfrac{2(1-\sigma)}{\varrho} \end{pmatrix}, \tag{4.3}$$

where the two relevant nondimensional parameters are the aspect ratio $\varrho = b/a$, and the Poisson ratio of the material σ. The friction contact surface is discretized into 33 nodes and set $\varrho = 0.5$ among all experiments.

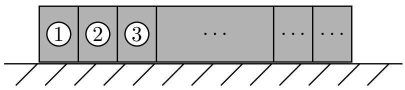

Figure 3. Unilateral friction contact system after discretization by finite element method.

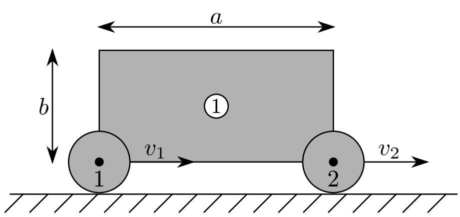

Figure 4. Diagram of the two-node element in impending slip to the right.

Node	υ	Node	υ	Node	υ
1	0.5366	12	0.0049	23	0.0074
2	0.3494	13	0.0032	24	0.0113
3	0.2275	14	0.0022	25	0.0174
4	0.1482	15	0.0016	26	0.0267
5	0.0965	16	0.0012	27	0.0409
6	0.0628	17	0.0011	28	0.0628
7	0.0409	18	0.0012	29	0.0965
8	0.0267	19	0.0016	30	0.1482
9	0.0174	20	0.0022	31	0.2275
10	0.0113	21	0.0032	32	0.3494
11	0.0074	22	0.0049	33	0.5366

Table 3. Values at the contact nodes with $\varrho = 0.5$, $\sigma = 0.05$ ($\delta = 1.3035$).

Node	$\sigma = 0.05$	$\sigma = 0.1$	$\sigma = 0.2$	$\sigma = 0.3$
1	0.5366	0.5467	0.5685	0.5927
2	0.3494	0.3467	0.3380	0.3233
3	0.2275	0.2199	0.2010	0.1763
4	0.1482	0.1394	0.1195	0.0962
5	0.0965	0.0884	0.0711	0.0525
6	0.0628	0.0561	00423	0.0286
7	0.0409	0.0356	0.0251	0.0156
8	0.0267	0.0226	0.0149	0.0085
9	0.0174	0.0143	0.0089	0.0046
10	0.0113	0.0091	0.0053	0.0025
11	0.0074	0.0058	0.0031	0.0014
12	0.0049	0.0037	0.0019	0.0008
13	0.0032	0.0024	0.0011	0.0004
14	0.0022	0.0016	0.0007	0.0002
15	0.0016	0.0011	0.0004	0.0001
16	0.0012	0.0008	0.0003	0
17	0.0011	0.0007	0.0003	0
18	0.0012	0.0008	0.0003	0
19	0.0016	0.0011	0.0004	0.0001
20	0.0022	0.0016	0.0007	0.0002
21	0.0032	0.0024	0.0011	0.0004
22	0.0049	0.0037	0.0019	0.0008
23	0.0074	0.0058	0.0031	0.0014
24	0.0113	0.0091	0.0053	0.0025
25	0.0174	0.0143	0.0089	0.0046
26	0.0267	0.0226	0.0149	0.0085
27	0.0409	0.0356	0.0251	0.0156
28	0.0628	0.0561	0.0423	0.0286
29	0.0965	0.0884	0.0711	0.0525
30	0.1482	0.1394	0.1195	0.0962
31	0.2275	0.2199	0.2010	0.1763
32	0.3494	0.3467	0.3380	0.3233
33	0.5366	0.5467	0.5685	0.5927

Table 4. Values of v at the contact nodes for different values of the Poisson ratio.

Table 3 displays the numerical values of the components at the contact nodes of the eigenmode represented in Figure 3, revealing that sliding occurs at each node and by calculation, r is equal to 0 at each node that the force at the corresponding node has not changed, which means that the equilibrium state of impending slip to the right of the 33 contact nodes has been reached.

The numerical values of υ at the contact nodes for different values of the Poisson ratio are shown in Table 4, which illustrates the transition from an all-slip mode to a non-all-slip mode occurring at nodes 16, 17, 18 as the Poisson ratio varies between 0.05 and 0.3. The corresponding values of δ are the following: $\delta = 1.3035$ for $\sigma = 0.05$, $\delta = 1.3618$ for $\sigma = 0.1$, $\delta = 1.4949$ for $\sigma = 0.2$, and $\delta = 1.6558$ for $\sigma = 0.3$. As the Poisson ratio of the material increases, so does the friction coefficient corresponding to its directional instability, which demonstrates the directional instability of the unilateral friction contact system in a quasi equilibrium state with different friction coefficients. The tables demonstrate the same pattern of variation as those calculated in literature [17], indicating that our method can be applied to calculate practical problems.

5. Conclusions

This paper delves into the fundamental properties of the symmetric Pareto EiCP. By using the structure and properties of the symmetric matrix, the symmetric Pareto EiCP can be transformed equivalently to the constrained optimization problem. Following that, the descent algorithms are proposed to solve the constrained optimization problem that utilizes the NCP function and the Rayleigh quotient gradient as descent direction and exact linear search to determine the step length. The numerical results show that our proposed algorithms improve the computational efficiency of solving symmetric Pareto EiCP. Furthermore, the algorithm is also extended to address the generalized eigenvalue complementarity problem arising from unilateral frictional elastic systems. However, there are many issues that require further investigation: One is how to improve the iterative efficiency and accuracy of the algorithm for larger-scale symmetric Pareto EiCP; the other is to delve deeper into the theory and properties of the algorithm, such as whether the corresponding algorithm can converge to the maximum (minimum) eigenvalue or part of the specified eigenvalue of the symmetric Pareto EiCP by selecting special initial values. The third question is how to apply existing theories and algorithms to asymmetric Pareto EiCP. We will use them as the next research topics in our future research.

References

[1] *S. Adly, H. Rammal*: A new method for solving Pareto eigenvalue complementarity problems. Comput. Optim. Appl. *55* (2013), 703–731. zbl MR doi

[2] *S. Adly, A. Seeger*: A nonsmooth algorithm for cone-constrained eigenvalue problems. Comput. Optim. Appl. *49* (2011), 299–318. zbl MR doi

[3] *G. P. Barker*: Theory of cones. Linear Algebra Appl *39* (1981), 263–291. zbl MR doi

[4] *C. P. Brás, A. Fischer, J. Júdice, K. Schönefeld, S. Seifert*: A block active set algorithm with spectral choice line search for the symmetric eigenvalue complementarity problem. Appl. Math. Comput. *294* (2017), 36–48. zbl MR doi

[5] *J.-S. Chen*: On some NCP-functions based on the generalized Fischer-Burmeister function. Asia-Pac. J. Oper. Res. *24* (2007), 401–420. zbl MR doi

[6] *J.-S. Chen, S. Pan*: A family of NCP functions and a descent method for the nonlinear complementarity problem. Comput. Optim. Appl. *40* (2008), 389–404. zbl MR doi

[7] *R. W. Cottle, J.-S. Pang, R. E. Stone*: The Linear Complementarity Problem. Computer Science and Scientific Computing. Academic Press, Boston, 1992. zbl MR doi

[8] *J. J. Júdice, M. Raydan, S. S. Rosa, S. A. Santos*: On the solution of the symmetric eigenvalue complementarity problem by the spectral projected gradient algorithm. Numer. Algorithms *47* (2008), 391–407. zbl MR doi

[9] *J. J. Júdice, H. D. Sherali, I. M. Ribeiro*: The eigenvalue complementarity problem. Comput. Optim. Appl. *37* (2007), 139–156. zbl MR doi

[10] *M. Kučera*: A new method for obtaining eigenvalues of variational inequalities: Operators with multiple eigenvalue. Czech. Math. J. *32* (1982), 197–207. zbl MR doi

[11] *V. K. Le*: Some global bifurcation results for variational inequalities. J. Differ. Equations *131* (1996), 39–78. zbl MR doi

[12] *H. A. Le Thi, M. Moeini, T. Pham Dinh, J. Júdice*: A DC programming approach for solving the symmetric eigenvalue complementarity problem. Comput. Optim. Appl. *51* (2012), 1097–1117. zbl MR doi

[13] *C. Ma*: The semismooth and smoothing Newton methods for solving Pareto eigenvalue problem. Appl. Math. Modelling *36* (2012), 279–287. zbl MR doi

[14] *J. A. C. Martins, A. Pinto Da Costa*: Stability of finite-dimensional nonlinear elastic systems with unilateral contact and friction. Int. J. Solids Struct. *37* (2000), 2519–2564. zbl MR doi

[15] *J. A. C. Martins, A. Pinto Da Costa*: Bifurcations and instabilities in frictional contact problems: Theoretical relations, computational methods and numerical results. European Congress on Computational Methods in Applied Sciences and Engineering, ECCOMAS 2004. University of Jyväskylä, Jyväskylä, 2004, pp. 102095.

[16] *A. Pinto Da Costa, J. A. C. Martins*: Computation of bifurcations and instabilities in some frictional contact problems. Available at `https://www.researchgate.net/publication/278629570_Computation_of_bifurcations_and_instabilities_in_some_frictional_contact_problems` (2001), 15 pages.

[17] *A. Pinto Da Costa, J. A. C. Martins, I. N. Figueiredo, J. J. Júdice*: The directional instability problem in systems with frictional contacts. Comput. Methods Appl. Mech. Eng. *193* (2004), 357–384. zbl MR doi

[18] *A. Pinto Da Costa, A. Seeger*: Cone-constrained eigenvalue problems: Theory and algorithms. Comput. Optim. Appl. *45* (2010), 25–57. zbl MR doi

[19] *M. Queiroz, J. Júdice, C. Humes, Jr.*: The symmetric eigenvalue complementarity problem. Math. Comput. *73* (2004), 1849–1863. zbl MR doi

[20] *P. Quittner*: Spectral analysis of variational inequalities. Commentat. Math. Univ. Carol. *27* (1986), 605–629. MR

[21] *A. Seeger*: Eigenvalue analysis of equilibrium processes defined by linear complementarity conditions. Linear Algebra Appl. *292* (1999), 1–14. zbl MR doi

[22] *A. Seeger, M. Torki*: On eigenvalues induced by a cone constraint. Linear Algebra Appl. *372* (2003), 181–206. zbl MR doi
[23] *A. Seeger, M. Torki*: Local minima of quadratic forms on convex cones. J. Glob. Optim. *44* (2009), 1–28. zbl MR doi
[24] *A. Seeger, J. Vicente-Perez*: On cardinality of Pareto spectra. Electron. J. Linear Algebra *22* (2011), 758–766. zbl MR doi
[25] *B.-S. Tam*: The Perron generalized eigenspace and the spectral cone of a cone-preserving map. Linear Algebra Appl. *393* (2004), 375–429. zbl MR doi
[26] *T. Zcghloul, B. Villechaise*: Stress waves in a sliding contact. Part 1: Experimental study. Tribology Series *31* (1996), 33–37. doi

Authors' address: *Lu Zou*, *Yuan Lei* (corresponding author), School of Mathematics, Hunan University, Lushan Road (S), Yuelu District, Changsha 410082, P. R. China, e-mail: `zoulu7@hnu.edu.cn`, `yleimath@hnu.edu.cn`.